

Aurora B activity is promoted by cooperation between discrete localization sites in budding yeast

Theodor Marsoner, Poornima Yedavalli, Chiara Masnovo, Sarah Fink, Katrin Schmitzer, and Christopher S. Campbell*

Department of Chromosome Biology, Max Perutz Labs, University of Vienna, A-1030 Vienna, Austria

ABSTRACT Chromosome biorientation is promoted by the four-member chromosomal passenger complex (CPC) through phosphorylation of incorrect kinetochore–microtubule attachments. During chromosome alignment, the CPC localizes to the inner centromere, the inner kinetochore, and spindle microtubules. Here we show that a small domain of the CPC subunit INCENP/Sli15 is required to target the complex to all three of these locations in budding yeast. This domain, the single alpha helix (SAH), is essential for phosphorylation of outer kinetochore substrates, chromosome segregation, and viability. By restoring the CPC to each of its three locations through targeted mutations and fusion constructs, we determined their individual contributions to chromosome biorientation. We find that only the inner centromere localization is sufficient for cell viability on its own. However, when combined, the inner kinetochore and microtubule binding activities are also sufficient to promote accurate chromosome segregation. Furthermore, we find that the two pathways target the CPC to different kinetochore attachment states, as the inner centromere-targeting pathway is primarily responsible for bringing the complex to unattached kinetochores. We have therefore discovered that two parallel localization pathways are each sufficient to promote CPC activity in chromosome biorientation, both depending on the SAH domain of INCENP/Sli15.

Monitoring Editor

Kerry Bloom
University of North Carolina,
Chapel Hill

Received: Nov 29, 2021

Revised: May 17, 2022

Accepted: Jun 9, 2022

INTRODUCTION

To faithfully segregate their chromosomes, eukaryotic cells form a bipolar spindle with microtubules from opposite spindle poles attached to each of the two sister chromatids. Microtubules bind to the centromere region of chromosomes via a multiprotein complex called the kinetochore. During chromosome alignment prior to anaphase, chromosomes transiently form many erroneous kinetochore–microtubule attachments where both sister chromatids are attached

to the same pole. To maintain a stable genome from one generation to the next, it is imperative that cells detect and correct such erroneous attachments.

During mitosis, kinetochore–microtubule misattachments are detected and corrected by the evolutionarily conserved chromosomal passenger complex (CPC). The CPC subunit Aurora B (Ipl1 in budding yeast) is a kinase that phosphorylates outer kinetochore substrates specifically on misattached chromosomes (Tanaka *et al.*, 2002; Lampson *et al.*, 2004; Cimini *et al.*, 2006; Welburn *et al.*, 2010). This phosphorylation decreases the affinity of the kinetochore for the microtubules, allowing for detachment followed by reattachment in the correct orientation (Sarangapani *et al.*, 2013). How the CPC targets to the outer kinetochore and how it specifically corrects misattachments are long-standing questions in the field (Lampson and Cheeseman, 2011; Krenn and Musacchio, 2015; Funabiki, 2019).

In addition to Aurora B/Ipl1, the CPC is composed of the subunits Survivin/Bir1, Borealin/Nbl1, and INCENP/Sli15. INCENP acts as a scaffold coordinating all of the CPC's activities. The N-terminus binds to Survivin and Borealin, the C-terminus binds to and activates Aurora B, and the central region of the protein directly interacts

This article was published online ahead of print in MBoC in Press (<http://www.molbiolcell.org/cgi/doi/10.1091/mbc.E21-11-0590>) on June 15, 2022.

*Address correspondence to: Christopher S. Campbell (christopher.campbell@univie.ac.at).

Abbreviations used: CIP, calf intestinal phosphatase; CPC, chromosomal passenger complex; DTT, dithiothreitol; FRB, FKBP12 rapamycin binding; HKMT, histone lysine methyltransferase; MTB, microtubule binding; PR, phosphoregulated; SAH, single alpha helix.

© 2022 Marsoner *et al.* This article is distributed by The American Society for Cell Biology under license from the author(s). Two months after publication it is available to the public under an Attribution–Noncommercial–Share Alike 4.0 International Creative Commons License (<http://creativecommons.org/licenses/by-nc-sa/4.0>).

“ASCB®,” “The American Society for Cell Biology®,” and “Molecular Biology of the Cell®” are registered trademarks of The American Society for Cell Biology.

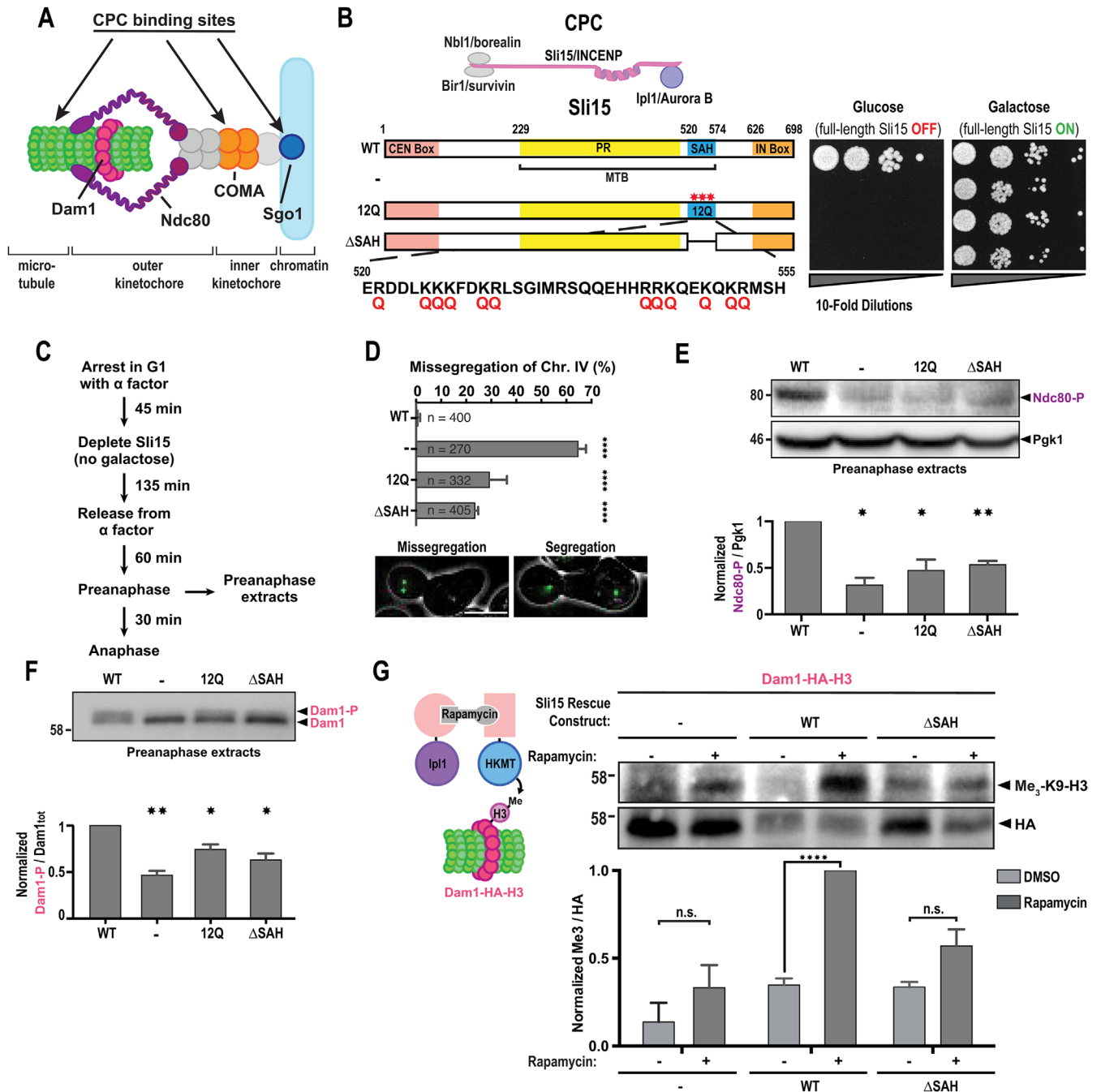


FIGURE 1: The SAH domain of Sli15 is essential for chromosome biorientation and outer kinetochore phosphorylation. (A) Schematic of a microtubule-bound kinetochore showing the CPC binding sites Sgo1 and COMA complex and the outer kinetochore substrates Ndc80 and Dam1. (B) Tenfold serial dilution analysis of cells constitutively expressing the indicated Sli15-SAH constructs with endogenous Sli15 under the control of a galactose-inducible promoter. Schematic on the left shows the 12 glutamine (Q) mutations in the SAH domain. (C) Protocol for Sli15 depletion in galactose-deficient media and synchronization of cells with subsequent release from G1-arrest into anaphase. (D) Mis-segregation rates for GFP-labeled Chr. IV of indicated Sli15 constructs during the first anaphase after endogenous Sli15 depletion according to the protocol in C. Representative images show a mis-segregation event (left) and a correct segregation event (right). Scale bar: 5 μm. Mean and SEM of at least three independent replicates are shown. (E) Immunoblotting analysis and quantification of Ndc80-S37 phosphorylation in preanaphase by the indicated Sli15 constructs. Cells were treated according to the protocol in C. Ndc80-P signal were first normalized to their respective Pgk1 signals and subsequently normalized to WT. Mean and SEM of three independent experiments are shown. (F) Immunoblotting analysis and quantification of Dam1 phosphorylation in preanaphase by the indicated Sli15 constructs. Cells were treated according to the protocol in C. Signal intensity of Phosphorylated Dam1 (Dam1-P) was divided by total Dam1 signal and subsequently normalized to WT. Mean and SEM of four independent replicates are shown. (G) Immunoblotting analysis and quantification for the amount of indicated Sli15 constructs in proximity to Dam1 in preanaphase. Dimerization of Ipl1-FRB and HKMT-FKBP12 was induced by addition of rapamycin 20 min after G1 release into

with microtubules. Accumulating evidence suggests that Aurora B localization to the inner centromere, the inner kinetochore, and spindle microtubules all contribute to substrate phosphorylation at the outer kinetochore (Figure 1A, reviewed in Krenn and Musacchio, 2015; Broad and DeLuca, 2020). Localization to the inner centromere is facilitated by interactions between INCENP, Survivin, and Borealin. This localization to the inner centromere is the predominant one observed during early mitosis and was long thought to be essential for the CPC's role in chromosome biorientation. However, we previously found that a deletion mutant of INCENP/Sli15 that eliminates the enrichment at the inner centromere is still able to undergo robust chromosome segregation in budding yeast (Campbell and Desai, 2013). Similarly, chicken cells bearing a survivin mutant that decreases centromeric CPC enrichment are viable (Yue *et al.*, 2008). Recently, similar perturbations in human cells have been shown to maintain high levels of outer kinetochore phosphorylation by the CPC (Hadders *et al.*, 2020). These results suggest the existence of other mechanisms for targeting the CPC to the outer kinetochore. Recent work has highlighted the importance of two additional localization sites for the CPC—at the inner kinetochore and at microtubules.

Inner kinetochore binding by the CPC has recently been implicated in promoting CPC function during chromosome segregation. In yeast, the CPC targets to the inner kinetochore directly via an interaction between Sli15 and the COMA complex (Fischböck-Halwachs *et al.*, 2019; García-Rodríguez *et al.*, 2019). In human cells, an active CPC pool located approximately 20 nm outside of the inner kinetochore protein CENP-C has been reported, although the direct binding partners at this location are currently unknown (Broad *et al.*, 2020). Additionally, recent evidence in frog egg extracts suggests that CPC binding to the inner kinetochore can contribute to kinetochore formation (Bonner *et al.*, 2019).

The role of microtubule binding (MTB) by the CPC in chromosome segregation has been demonstrated by examining the INCENP MTB domain. INCENP homologues contain a region directly upstream of the Aurora B-binding IN box that is predicted to form a single alpha helix (SAH) (Peckham and Knight, 2009; van der Horst and Lens, 2013). This region in chicken INCENP has been confirmed to be a SAH biochemically and also binds directly to microtubules *in vitro* (Samejima *et al.*, 2015). In human cell culture, the SAH domain contributes to centromere localization, kinetochore phosphorylation, and mitotic checkpoint activation (Vader *et al.*, 2007; Wheelock *et al.*, 2017).

In the budding yeast *Saccharomyces cerevisiae*, the predicted SAH is part of a larger MTB domain in the central region of Sli15 (Kang *et al.*, 2001). In addition to the SAH, the MTB domain contains a phosphoregulated (PR) region whose MTB activity is suppressed by Cdk1 phosphorylation (Figure 1B). At anaphase onset, the PR region is dephosphorylated by Cdc14 and the CPC relocates from the inner centromere to the microtubules of the mitotic spindle (Pereira, 2003). We have previously shown that the MTB domain is essential for CPC function in chromosome biorientation in budding yeast. However, the Cdc14-dependent spindle localization occurs after chromosome biorientation has completed, indicating that there is an additional role of the MTB domain that is responsible for its essential function in chromosome segregation (Fink *et al.*, 2017). It is currently unknown if the essential function of the MTB domain is in MTB or some other activity.

Two recent studies have demonstrated that the inner centromere and the inner kinetochore CPC targeting mechanisms are at least partially redundant for chromosome biorientation and cell viability in budding yeast (Fischböck-Halwachs *et al.*, 2019; García-Rodríguez *et al.*, 2019). These results demonstrate the presence of two separable targeting pathways. In this study, we aimed to answer three key questions relating to the function of the CPC in these two pathways: 1) are either of these pathways dependent on the Sli15 SAH domain and its MTB activity? 2) Do the two pathways preferentially target different types of misattachments? 3) Are any of the three CPC targeting mechanisms (inner centromere, inner kinetochore, or microtubules) entirely sufficient for chromosome biorientation?

We find that SAH mutants have reduced outer kinetochore phosphorylation, increased rates of chromosome missegregation, and are inviable. Surprisingly, mutations in the SAH domain prevent CPC localization to all known regions in budding yeast—microtubules, the inner centromere, and the inner kinetochore. By restoring targeting of the CPC to each of these regions individually, we determined the contributions of these binding activities to CPC function. We find that inner centromere binding of the CPC is sufficient to partially rescue viability, whereas inner kinetochore binding only rescues in combination with increased MTB. Furthermore, we find that under conditions where the microtubules have been depolymerized, only the inner centromere-targeting pathway is active. Our results are consistent with a model based on two pathways, with the inner centromere pathway primarily active at unattached kinetochores and the inner kinetochore plus MTB pathway only active at misattached kinetochores.

RESULTS

The SAH domain of Sli15 is essential for chromosome biorientation

A conserved feature of INCENP homologues is a predicted SAH domain directly upstream of the IN box (van der Horst and Lens, 2013). We previously demonstrated that dimerization of a truncation mutant comprising the SAH and IN box of the *S. cerevisiae* INCENP homolog Sli15 rescues CPC function, indicating that this relatively short construct is sufficient to fulfill all essential functions of Sli15 (Fink *et al.*, 2017). Additionally, Sli15 constructs that only contain the IN box are inviable, demonstrating the importance of the SAH. These results prompted us to determine how mutations that specifically disrupt the short SAH domain of Sli15 affect CPC function. To test this, we engineered Sli15 mutants that either fully delete this region (Sli15-ΔSAH) or contain point mutations in which 12 conserved basic residues in the SAH were changed to glutamines (Sli15-12Q) in order to reduce the strong net positive charge of this region without disrupting the predicted helical fold (van der Horst *et al.*, 2015; Figure 1B; Supplemental Figure S1A). Expression of the mutant constructs was confirmed by Western blot, although the Sli15-12Q mutant was expressed at lower levels compared with the other constructs (Supplemental Figure S1B). After depletion of endogenous Sli15 via a galactose inducible promoter, both the Sli15-12Q and the Sli15-ΔSAH constructs failed to rescue viability, indicating that the SAH domain and its positively charged amino acids are essential for CPC function (Figure 1B). Additionally, both mutant constructs were lethal when overexpressed in a wild-type background, suggesting they act in a dominant negative manner to impair CPC function (Supplemental Figure S1C). As chromosome biorientation

metaphase arrest by depleting Cdc20. Dam1 proximity was assessed via an antibody recognizing trimethylated peptide H3 on Lysine 9. HA-epitope present on the signaling peptide served as an internal loading control. Quantification shows the mean and SEM of three independent experiments. * $p < 0.05$, ** $p < 0.01$, *** $p < 0.001$, **** $p < 0.0001$.

is the only known essential function of the CPC in budding yeast, we next measured chromosome segregation rates of Sli15-12Q and Sli15- Δ SAH (Biggins *et al.*, 1999). Cells were synchronized in G1 and endogenous Sli15 was depleted before subsequent release into the cell cycle (Figure 1C). In the first cell division following Sli15 depletion, GFP-labeled chromosome IV was missegregated 62% of the time. Expression of Sli15-12Q or Sli15- Δ SAH only reduced missegregation rates to 29 and 23%, respectively (Figure 1D). These missegregation rates are consistent with the observed lethality, as we previously observed that missegregation rates of ~5% per chromosome are sufficient to severely impair growth (Ravichandran *et al.*, 2018). In addition to missegregation rates, we directly measured chromosome biorientation in preanaphase using GFP-labeled chromosome IV (Tanaka *et al.*, 2002; Makrantonis and Stark, 2009). Consistent with the missegregation rates, cells containing Sli15- Δ SAH showed reduced chromosome biorientation early in mitosis (60 min after release from G1; Supplemental Figure S1D). We conclude that the SAH domain of Sli15 is essential for viability and faithful chromosome segregation.

The SAH domain of Sli15 is essential for outer kinetochore phosphorylation

The CPC facilitates chromosome biorientation by phosphorylating the outer kinetochore complexes Ndc80 and Dam1, which form direct kinetochore–microtubule attachments (Cheeseman *et al.*, 2002, 2006; DeLuca *et al.*, 2006; Sarangapani *et al.*, 2013). We hypothesized that the high chromosome missegregation rates could result from an inability of the SAH mutants to phosphorylate Ndc80 and Dam1. Ipl1-dependent kinetochore phosphorylation levels are high early in mitosis and decrease as cells become bioriented in metaphase (Keating *et al.*, 2009; DeLuca *et al.*, 2011). We defined the early “preanaphase” stage based on the timing of the separation of chromosome IV and the degradation of Pds1/securin (Supplemental Figure S1E). To detect Ipl1 phosphorylation of the kinetochore, we generated a phosphospecific antibody that recognizes phosphorylated serine 37 on Ndc80 and measured the signal by western blot (Figure 1E and Supplemental Figure S1F). In addition, we measured the phosphorylation-dependent mobility shift of Dam1 (Storchova *et al.*, 2011; Fink *et al.*, 2017). After synchronization and depletion of endogenous Sli15 in G1, we released the cells from the arrest and prepared preanaphase extracts (Figure 1C). Immunoblotting showed significantly decreased Ndc80 and Dam1 phosphorylation in cells expressing the Sli15-12Q and Sli15- Δ SAH mutants (Figure 1, E and F). By contrast, phosphorylation of the conserved Aurora B/Ipl1 substrate Histone H3 on serine 10 (H3-S10) was not reduced with Sli15- Δ SAH, demonstrating that global Ipl1 kinase activity is not negatively impacted (Supplemental Figure S1G). H3-S10 phosphorylation by Sli15-12Q was slightly reduced, which is consistent with the reduced expression levels of this construct. Together, these results demonstrate that the SAH domain of Sli15 is required specifically for outer kinetochore phosphorylation by the CPC to ensure faithful chromosome segregation and viability.

The SAH domain of Sli15 is essential for outer kinetochore proximity of the CPC

Decreased phosphorylation of outer kinetochore CPC substrates could result either from reduced proximity or from diminished kinase activation specifically at that location. To differentiate between these two possibilities, we used the M-track protein-protein proximity assay. This method does not rely on CPC activity, which allowed us to test if the SAH domain is necessary for either active or inactive CPC to come in close proximity with its outer kinetochore substrates

(Zuzuarregui *et al.*, 2012; Brezovich *et al.*, 2015). Ipl1 was bound to human histone lysine methyltransferase (HKMT) via the rapamycin inducible FRB-FKBP12 dimerization system. A short peptide from a HKMT substrate, histone H3, was fused to Dam1 (Dam1-H3). This peptide is irreversibly trimethylated if Ipl1-HKMT comes in close proximity (Figure 1G). CPC proximity to the outer kinetochore was determined by immunoblot using an antibody that specifically recognizes trimethylated histone H3 (Me₃-K9-H3). Although the methylation site (K9) in this peptide is adjacent to an Ipl1 phosphorylation site (S10) within H3, methylation efficiency of this peptide was indistinguishable from an S10A mutant peptide (data not shown). Importantly, phosphorylation of the H3 tag on S10 did not impair the binding of the Me₃-K9-H3 antibody, as there was no detectable difference in the trimethylation signal in extracts following treatment with calf intestinal phosphatase (CIP; Supplemental Figure S1H). A trimethylation signal was readily observed on Dam1-H3 in the wild-type Sli15 strain in preanaphase on the addition of rapamycin. By contrast, expression of Sli15- Δ SAH did not show increased methylation when compared with Sli15 depletion alone, demonstrating that the SAH is necessary for CPC proximity to the outer kinetochore (Figure 1G). However, it is possible that in addition to impaired outer kinetochore proximity, Ipl1 kinase activation is also decreased in the Sli15- Δ SAH mutant. The spatial resolution of the M-track assay was assessed by fusing HKMT to the centromeric protein Ndc10, which showed a strong trimethylation signal with the inner kinetochore protein Mif2-H3 but no increase in trimethylation signal with Dam1. We therefore conclude that the M-track assay can distinguish between proximity to the inner versus outer kinetochore (Supplemental Figure S1I). Collectively, our results show that the SAH domain and its positively charged amino acids are essential for viability, faithful chromosome segregation, outer kinetochore phosphorylation, and Dam1 proximity.

The SAH domain of Sli15 is essential for all of its preanaphase localization activities

The CPC has been demonstrated to bind to the inner centromere, the inner kinetochore, and microtubules, and all three of these localization activities have been proposed to contribute to chromosome biorientation (reviewed in Broad and DeLuca, 2020). To investigate which of these localizations is disrupted in the SAH mutants, we labeled the Sli15 constructs with mNeonGreen and observed their localization in preanaphase, when chromosome biorientation occurs. Preanaphase spindles were classified as shorter than 2 μ m and being located entirely in the mother cell. Localization of Sli15 to the spindle is almost completely absent in the SAH mutant cells (Figure 2A). The SAH deletion also disrupted the spindle localization of the Bir1 subunit of the CPC (Supplemental Figure S2A). We note that due to the small size of the budding yeast spindle, these measurements were conducted in an area that includes the spindle microtubules, kinetochores, and the inner centromere. This strong disruption of localization was largely confined to prometaphase, as localization to the anaphase spindle was only decreased by ~30–40% (Figure 2B; Supplemental Figure S2A).

These data suggest that all of the observable preanaphase CPC targeting activities require a functional SAH domain. This includes microtubule targeting via the Sli15 MTB domain, inner kinetochore targeting through the Ctf19 subunit of the COMA complex, and inner centromere targeting through Sgo1. MTB activity of the chicken and human INCENP SAH domains has also been directly demonstrated *in vitro* (Samejima *et al.*, 2015; van der Horst *et al.*, 2015). However, the SAH of Sli15 is considerably shorter and comprises only a small part of the MTB domain of INCENP. To determine

whether the SAH contributes to the MTB activity of the MTB in yeast, we expressed and purified wild-type and mutant MTB domains from *Escherichia coli*. When incubated with taxol-stabilized microtubules and centrifuged at high speed, there was an ~20% decrease in the amount of MBP-MTB-12Q and MBP-MTB-ΔSAH in the pellet when compared with wild type. This indicates that the SAH domain contributes to MTB in vitro, although not as strongly as the PR region of the MTB (Supplemental Figure S2B). We note that the PR region of the purified protein is likely in an unphosphorylated state, similar to that present in anaphase and therefore has strong MTB affinity independently of the SAH. The decreased MTB for the SAH mutants in vitro is consistent with the decrease in anaphase spindle localization measured in vivo (Figure 2B).

The lack of any observable localization at the spindle/kinetochore would imply that the binding to Ctf19 at the inner kinetochore is also disrupted in the absence of a functional SAH domain. This could result from the Sli15-12Q and Sli15-ΔSAH directly affecting the binding between the CPC and the Ctf19 subunit of the COMA complex. The interaction between Ctf19 and Sli15 has been mapped to two regions that flank the SAH, which suggests that this would be possible (Fischböck-Halwachs *et al.*, 2019). Alternatively, the reduction in MTB could indirectly affect the ability of the complex to interact with the inner kinetochore.

Although the CPC localizes strongly to microtubules in anaphase, the CPC predominantly localizes to the inner centromere during chromosome biorientation in both yeast and human cells (Ainsztein *et al.*, 1998; Klein *et al.*, 2006; Campbell and Desai, 2013). It was surprising that disruption of the SAH abolished inner centromere localization, as the centromere-targeting region (CEN box) of Sli15 is not located close to the SAH in the primary sequence of the protein (Figure 1B). However, similar observations were made in *Xenopus* egg extracts and human cells, where chromatin localization was decreased in the absence of the SAH (Wheelock *et al.*, 2017). We tested if the CEN box is still able to form an intact CPC complex in the ΔSAH mutant by observing Bir1-mNeonGreen localization to the anaphase spindle. After Sli15 depletion, the Sli15-ΔSAH mutant was capable of restoring Bir1 localization to a similar extent as observed directly for mNeonGreen-Sli15-ΔSAH, demonstrating that the CEN box of Sli15 is still able to form an intact complex (compare Figures 2B and Supplemental Figure S2A). We next looked further upstream in the localization pathway at Sgo1, which recruits the CPC to the inner centromere. The CPC in turn has been shown to promote Sgo1 localization at the inner centromere in frog egg extracts, flies, and human cells (Dai *et al.*, 2006; Resnick *et al.*, 2006; Boyarchuk *et al.*, 2007). We therefore hypothesized that the SAH may contribute to the positive feedback loop between the CPC and the Sgo1 to promote centromere-proximal recruitment. We monitored Sgo1-mNeonGreen recruitment after depletion of Sli15 and rescued with either wild-type Sli15 or Sli15-ΔSAH. The number of cells with Sgo1 between the kinetochore clusters at the inner centromere is greatly diminished in the ΔSAH mutant (Figure 2C). This suggests that Sgo1 centromeric recruitment is promoted by the CPC in yeast, and that the SAH domain is required for this activity. In the absence of inner centromere localization in the Sli15 mutants, Sgo1 was instead observed largely either in the vicinity of the kinetochores or proximal to the spindle pole bodies (SPBs; Supplemental Figure S2C). This localization was surprising, since there is no known function of Sgo1 near the SPBs. This enrichment of Sgo1 near the SPBs could result from an increase in the number of centromeres proximal to this location (Jin *et al.*, 2000). However, we did not observe any increase in centromeres located outside of the kinetochore foci in either Sli15-ΔSAH or Sli15 depletion (Supplemental

Figure S2D). Intriguingly, the CPC was also not observed at the SPBs in the Sli15-ΔSAH mutant (Figure 2A), indicating that Sgo1 does not interact with the CPC at this location.

The lack of any observable localization for the CPC in the SAH mutants suggests that disruption of the SAH abolishes all localization activities of the CPC. However, due to the small size of the preanaphase spindle, it is difficult to distinguish between each of the CPC locations on the spindle/chromosomes. We therefore used targeted mutations that disrupt CPC recruitment to the inner centromere or inner kinetochore and quantitatively compared them to the Sli15-ΔSAH mutant. Deletion of either Sgo1 or Ctf19 each decreased CPC spindle/chromosome localization by ~50% in preanaphase (Figure 2D). By comparison, deletion of the SAH decreased fluorescence by ~90%. Simultaneous removal of Ctf19 and Sgo1 by deletion and depletion, respectively, still resulted in more CPC spindle/chromosome fluorescence than Sli15-ΔSAH. This residual signal in the double deletion/depletion strain is potentially due to the MTB activity of the SAH. We conclude that in addition to MTB, the SAH domain of Sli15 is necessary to target the CPC to the inner centromere and the inner kinetochore prior to anaphase.

The SAH domain of Sli15 has functions that are independent of MTB

The SAH domain of INCENP has primarily been found to function in MTB (Tseng *et al.*, 2010; Samejima *et al.*, 2015; van der Horst *et al.*, 2015; Wheelock *et al.*, 2017). Although we observed that all CPC localizations to the spindle/chromosomes are dependent on the SAH domain, it is possible that all of these localizations depend on the interaction with microtubules. We therefore wanted to determine if the role of the SAH in targeting the CPC to the inner centromere or inner kinetochore was dependent on its MTB activity. We depolymerized microtubules using a combination of nocodazole and benomyl (Campbell and Desai, 2013; Verzijlbergen *et al.*, 2014). The combination of drugs was used because high concentrations of nocodazole alone are insufficient to efficiently depolymerize microtubules in budding yeast (Gillett *et al.*, 2004). With the nocodazole and benomyl concentrations used in our experiments, we observed a twofold increase in spindle assembly checkpoint (SAC) protein Bub3-mNeonGreen signal at prometaphase kinetochores compared with DMSO-treated control cells (Supplemental Figure S2E). Additionally, the nocodazole and benomyl treatment reduced mNeonGreen-Tub1 signals by 90%, indicating that the majority of microtubules were depolymerized (Supplemental Figure S2E). We conclude that the nocodazole/benomyl treatment increases the number of unattached kinetochores and nearly eliminates the presence of microtubules. To determine the effect of the SAH on CPC localization in the absence of microtubules, cells were synchronized and 45 min after release from a G1 arrest, microtubules were depolymerized with nocodazole/benomyl for 15 min. CPC localization was assessed in prometaphase cells 60 min after G1 release. We observed a ~3-fold enrichment of the CPC between the two kinetochore clusters on drug treatment compared with the DMSO control (Figure 2E). These measurements are in line with published experiments demonstrating that the CPC localization to chromosomes increases in the presence of unattached kinetochores (Knowlton *et al.*, 2006; Salimian *et al.*, 2011; Campbell and Desai, 2013). This chromatin enrichment of the CPC was undetectable in Sli15-ΔSAH mutant cells, similar to what we observed for this mutation in the presence of microtubules (Figure 2E). Nuf2 signal intensity, on the other hand, was unaffected by either Sli15 depletion or the Sli15-ΔSAH mutant, demonstrating that kinetochore formation still occurred normally (Figure 2E). The SAH is therefore also required for the

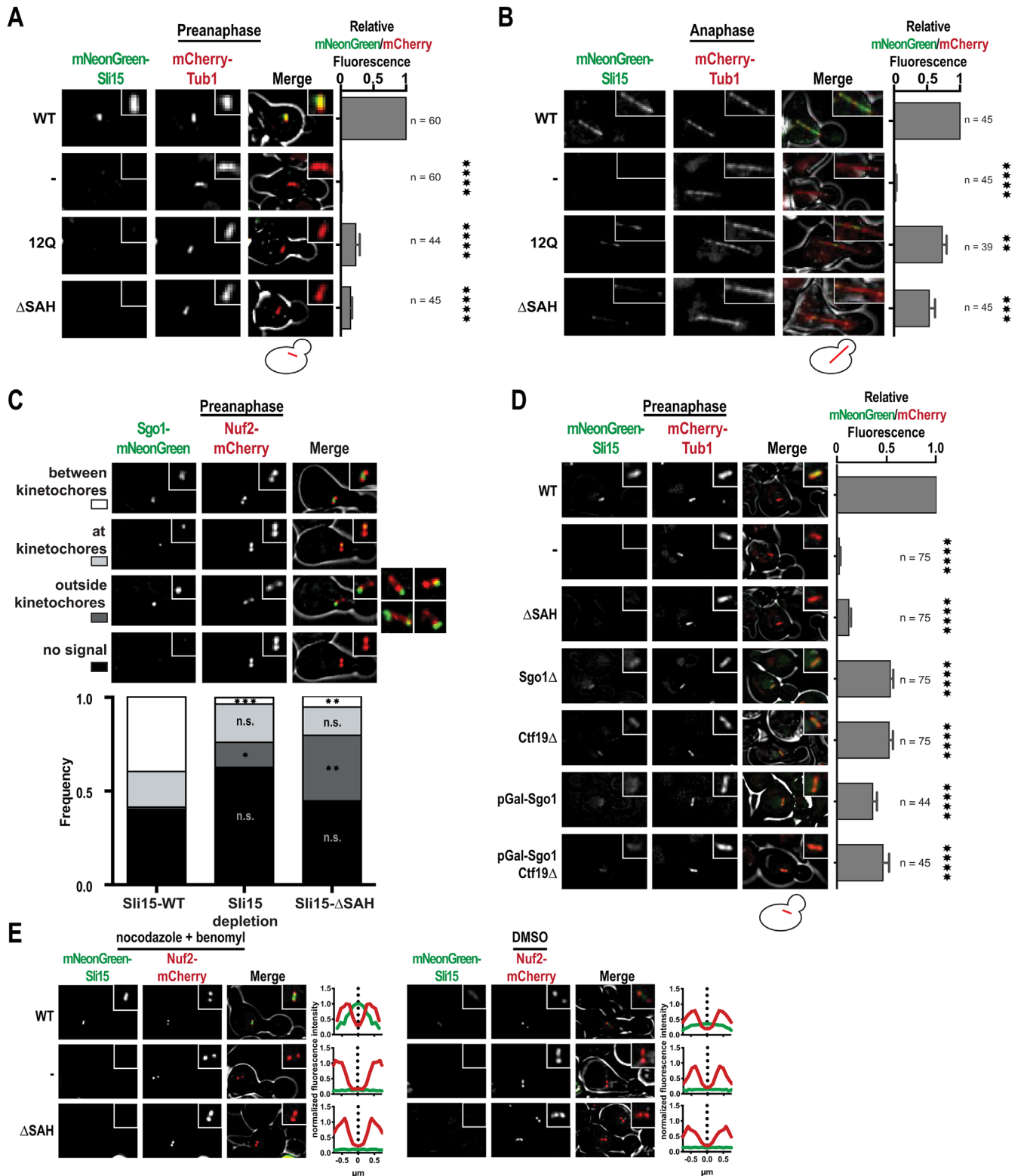


FIGURE 2: The SAH domain of Sli15 is required for CPC localization to microtubules, the inner kinetochore and the inner centromere. (A) Spindle localization of Sli15 constructs in preanaphase. Preanaphase spindles were defined as shorter than 2 μ m and located entirely in the mother cell. Images of the same fluorophore were contrast adjusted identically. Spindle localization was quantified by fitting and integrating a Gaussian curve to the signal intensity profile of a line drawn perpendicular to the spindle. Mean and SEM from at least three independent experiments are shown. For the values of individual fluorophores, see Supplemental Table S1. Insert box: 2 μ m square. **** p < 0.0001. (B) Spindle localization of Sli15 constructs in anaphase. Quantification of spindle localization was performed as in A. Mean and SEM from three independent experiments are shown. Insert box: 6.25 μ m in length. * p < 0.05. (C) Example images and quantification of Sgo1 localization in preanaphase. Sgo1 localization was classified into no signal, between, at, or

enrichment of the CPC at chromosomes with unattached kinetochores, demonstrating a role for the domain that is independent of MTB.

Inner centromeric Sgo1 binding is the predominant CPC recruitment pathway at unattached kinetochores

We next wanted to test the degree to which each of the two recruitment pathways is responsible for CPC localization to unattached kinetochores. In human cells, the increase in CPC localization to unattached kinetochores is partially dependent on Sgo1 recruitment via signaling from the kinase Mps1 (van der Waal *et al.*, 2012). In yeast, Sgo1 is enriched at the inner centromeres of chromosomes with unattached kinetochores (Nerusheva *et al.*, 2014). Whether the Ctf19-dependent recruitment pathway contributes to enrichment at unattached kinetochores is unknown. To test this, we measured the CPC levels in nocodazole/benomyl-treated cells with either the depletion of Sgo1, deletion of Ctf19, or both. Quantification of mNeonGreen-Sli15 signals revealed that Sgo1 depletion reduced CPC enrichment near the kinetochores to levels similar to those observed in the Sli15- Δ SAH. We conclude that the Sgo1-dependent inner centromere targeting is the predominant CPC localization mechanism at unattached kinetochores (Figure 3A).

By contrast with Sgo1 depletion, Ctf19 deletion had no measurable effect on CPC levels near unattached kinetochores either alone or in combination with Sgo1 depletion (Figure 3A). This suggests that the Ctf19-dependent inner kinetochore CPC localization requires the presence of microtubules. One possibility for this dependency is that the MTB activity of the CPC is required for targeting the complex to the inner kinetochore. This theory would also explain why mutations in the SAH domain do not have any observable localization to the inner kinetochore, as the MTB of the SAH domain could indirectly contribute to the inner kinetochore localization. The lack of any measurable contribution of Ctf19 to CPC localization at unattached kinetochores also suggests that the inner kinetochore CPC recruitment pathway acts specifically at misattached (syntelic) kinetochores.

In addition to observing CPC localization with fluorescence microscopy, we used the M-track assay to measure the amount of Ipl1 in proximity to the cohesin subunit Mcd1 at chromatin near the centromere/kinetochore. Cohesin is enriched near centromeres during chromosome alignment and should be proximal to both the inner centromere and the inner kinetochore (Waizenegger *et al.*, 2000; Warren *et al.*, 2000). In agreement with the microscopy measurements, Ctf19 or Sgo1 deletion reduced CPC targeting to the pericentromeric chromatin to a similar degree in unsynchronized cells compared with wild-type controls. However, in cells arrested with nocodazole and benomyl treatment, a decrease in CPC targeting to pericentromeric chromatin was only observed in the absence of Sgo1 but not in the absence of Ctf19 (Figure 3B). This observation is consistent with the microscopy measurements, as both assays showed that Ctf19 deletion only decreased CPC signal in the presence of microtubules, whereas Sgo1 deletion showed reduced CPC

localization in both the presence or the absence of microtubules (Figure 3B). To determine if this Sgo1-dependent decrease in CPC localization correlates with a decreased activity at the outer kinetochore, we measured the phosphorylation of Ndc80 as in Figure 1E. Ndc80 phosphorylation increased in the presence of nocodazole and benomyl as shown by a ratio of treated to untreated cells of ~ 1.25 . This increase was dependent on Sgo1 and the SAH domain of Sli15. However, this response in outer kinetochore phosphorylation following microtubule depolymerization was not negatively affected by deletion of Ctf19 (Figure 3C). Together, these results demonstrate that both inner kinetochore and inner centromere targeting of the CPC contribute to its localization and kinetochore phosphorylation activity in the presence of microtubules. However, the Sgo1-dependent inner centromere targeting becomes primarily responsible for both CPC enrichment at the inner centromere and outer kinetochore phosphorylation in the absence of microtubules. This appears to result from a combination of increased inner centromeric recruitment to unattached kinetochores and decreased inner kinetochore recruitment in the absence of microtubules.

Inner centromeric CPC recruitment is sufficient for chromosome biorientation

Although the presence of either the Sgo1-dependent inner centromere recruitment pathway or the Ctf19-dependent inner kinetochore recruitment pathway is essential for viability, whether either of these two pathways is entirely sufficient is unknown. The lack of any observable localization of the CPC in preanaphase for the SAH mutants presented us with an opportunity to individually restore targeting activities and determine which localizations are sufficient for CPC function in chromosome biorientation. We therefore sought to determine if inner centromere, inner kinetochore, or microtubule targeting could restore error correction (Figure 4A). We fused full-length Sli15 or the Sli15- Δ SAH mutant to Sgo1 or Okp1 (part of the COMA complex) to restore inner centromere or inner kinetochore localization, respectively. To increase Sli15 association with microtubules, we mutated six Cdk1 phosphorylation sites in the PR region to unphosphorylatable alanines (Sli15-6A; Figure 4A). These mutations have been shown to prematurely target the CPC to mitotic spindle microtubules prior to anaphase. Importantly, the 6A mutant does not affect cell cycle timing, chromosome missegregation rates, or viability (Pereira, 2003; Mirchenko and Uhlmann, 2010). All three targeting methods restored localization of the Sli15- Δ SAH to different positions along the spindle/chromosomes (Figure 4B). As expected, the 6A, Δ SAH double mutant localizes to the entire spindle/chromosomes, even more than wild-type Sli15. The Sgo1- Δ SAH construct localizes primarily between the two kinetochores, indicating that the fusion construct is sufficient to restore the ability of the CPC to promote the inner centromeric localization of Sgo1. The Okp1- Δ SAH fusion fully colocalizes with kinetochores. Each artificial targeting mechanism is therefore capable of localizing the CPC to a distinct region of the spindle/chromosomes consistent with the predicted location.

outside Nuf2-mCherry. Mean of three independent measurements are shown. Insert box: 2.5 μ m square. * $p < 0.05$; ** $p < 0.01$; *** $p < 0.001$. (D) Spindle localization of mNeonGreen-Sli15 in preanaphase with the indicated depletions, deletions, or mutants. Quantification was performed as in A. Mean and SEM of at least three independent experiments are shown. Insert box: 2.2 μ m square. **** $p < 0.0001$ (E) Inner centromere localization of mNeonGreen-WT and mNeonGreen- Δ SAH was determined in preanaphase after 15 min of treatment with nocodazole and benomyl or DMSO. Nuf2-mCherry signal was used to determine the mitotic stage. Images of the same fluorophore are contrast adjusted the same. Insert box: 2.4 μ m square. Enrichment of Sli15 constructs was analyzed by drawing a line along the spindle axis using the Nuf2-mCherry signals as reference points. The intensities of mCherry and mNeonGreen signals of 20 cells were averaged and normalized to WT in nocodazole/benomyl.

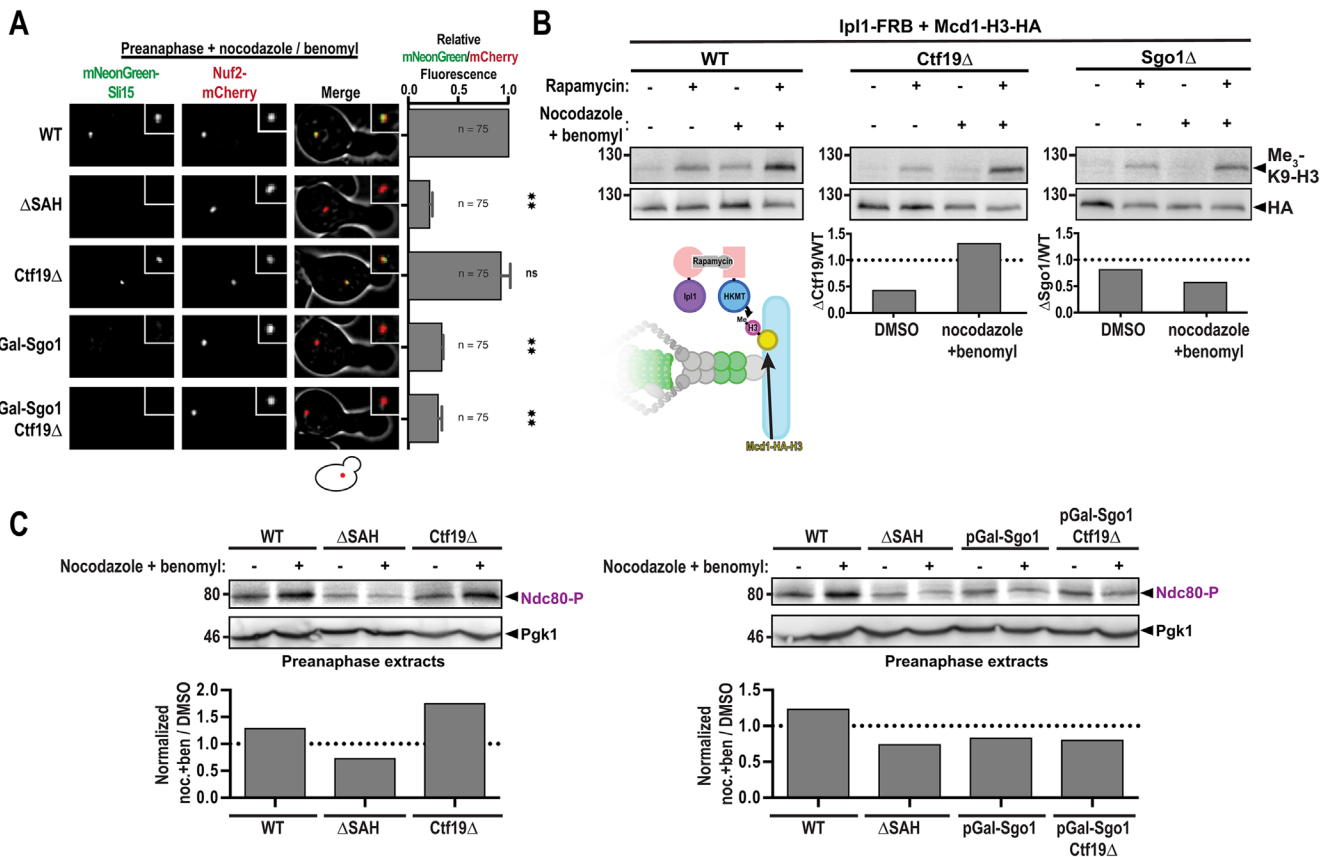


FIGURE 3: The inner centromere localization pathway is primarily responsible for CPC enrichment near unattached kinetochores. (A) Localization of mNeonGreen-Sli15 in preanaphase after 20 min incubation with nocodazole and benomyl in combination with indicated depletions, deletions, or mutants. Nuf2-mCherry signals appear as single dots due to spindle collapse induced by prolonged nocodazole and benomyl treatment. Mean and SEM from three independent experiments are shown. (B) Immunoblot analysis and quantification for the proximity of indicated Sli15 constructs to Mcd1 in unsynchronized cells. Dimerization of Ipl1-FRB and HKMT-FKBP12 was induced by addition of rapamycin. Mcd1 proximity was assessed via an antibody recognizing trimethylated peptide H3 on Lysine 9 (Me₃-K9-H3). The HA-epitope present on the signaling peptide served as an internal loading control. For quantifications H3 signals were first divided by their respective HA signals and then normalized to WT. Averages of two independent experiments are shown. (C) Immunoblotting analysis of Ndc80-S37 in preanaphase by the indicated Sli15 constructs, deletions, and depletions; 45 min after G1 release cells were either treated with nocodazole and benomyl (noc+ben) or DMSO. Cells were treated as depicted in Figure 1C and harvested in preanaphase. Each Ndc80-P signal was first normalized to Pgk1 and then ratios of noc +ben/DMSO were calculated.

To determine whether tethering of different Sli15 mutants to the inner centromere, inner kinetochore, or microtubules would rescue CPC function, the viability of these chimeras was tested in Sli15-depleted cells. Fusion of Sgo1 to Sli15-ΔSAH led to a partial rescue of viability and a large reduction in the chromosome missegregation rate (Figures 4C and Supplemental Figure S3A). Surprisingly, the rescue of chromosome missegregation did not lead to a rescue in Ndc80 phosphorylation, suggesting that inner centromere localization of the CPC has additional functions other than Ndc80 phosphorylation (Supplemental Figure S3B). These data suggest that recruitment of the CPC to the inner centromere is sufficient to promote biorientation. In contrast with the Sgo1 fusion, fusion of Sli15-ΔSAH to Okp1 neither rescued viability nor chromosome missegregation (Figures 4C and Supplemental Figure S3A). Surprisingly, Okp1-ΔSAH did, however, rescue Ndc80 phosphorylation, suggesting that bringing Ipl1 activity closer to the outer kinetochore is sufficient for outer kinetochore phosphorylation but additional functions are necessary to rescue chromosome segregation (Supplemental Figure S3B). We conclude that inner centromere tar-

geting, but not inner kinetochore targeting, is sufficient for CPC function.

CPC MTB leads to tension-independent kinetochore phosphorylation

We next looked at the effect of restoring MTB on CPC function. Cells expressing mutations that restore spindle association in the absence of a functional SAH (Sli15-6A,12Q or Sli15-6A,ΔSAH) were not viable following depletion of endogenous Sli15 (Figure 4C and Supplemental Figure S3C). Similar to what was observed for Okp1-ΔSAH, the Sli15-6A,ΔSAH and Sli15-6A,12Q double mutants were able to partially restore Ndc80 phosphorylation and Dam1 phosphorylation in preanaphase (Supplemental Figure S3D). To determine how the increased MTB could restore CPC activity but not viability, we first determined if the lethality was associated with high rates of chromosome missegregation. The chromosome missegregation rates of the Sli15-6A,12Q and Sli15-6A,ΔSAH constructs were similar to those of the Sli15-12Q and Sli15-ΔSAH constructs, indicating that increased kinetochore phosphorylation does not

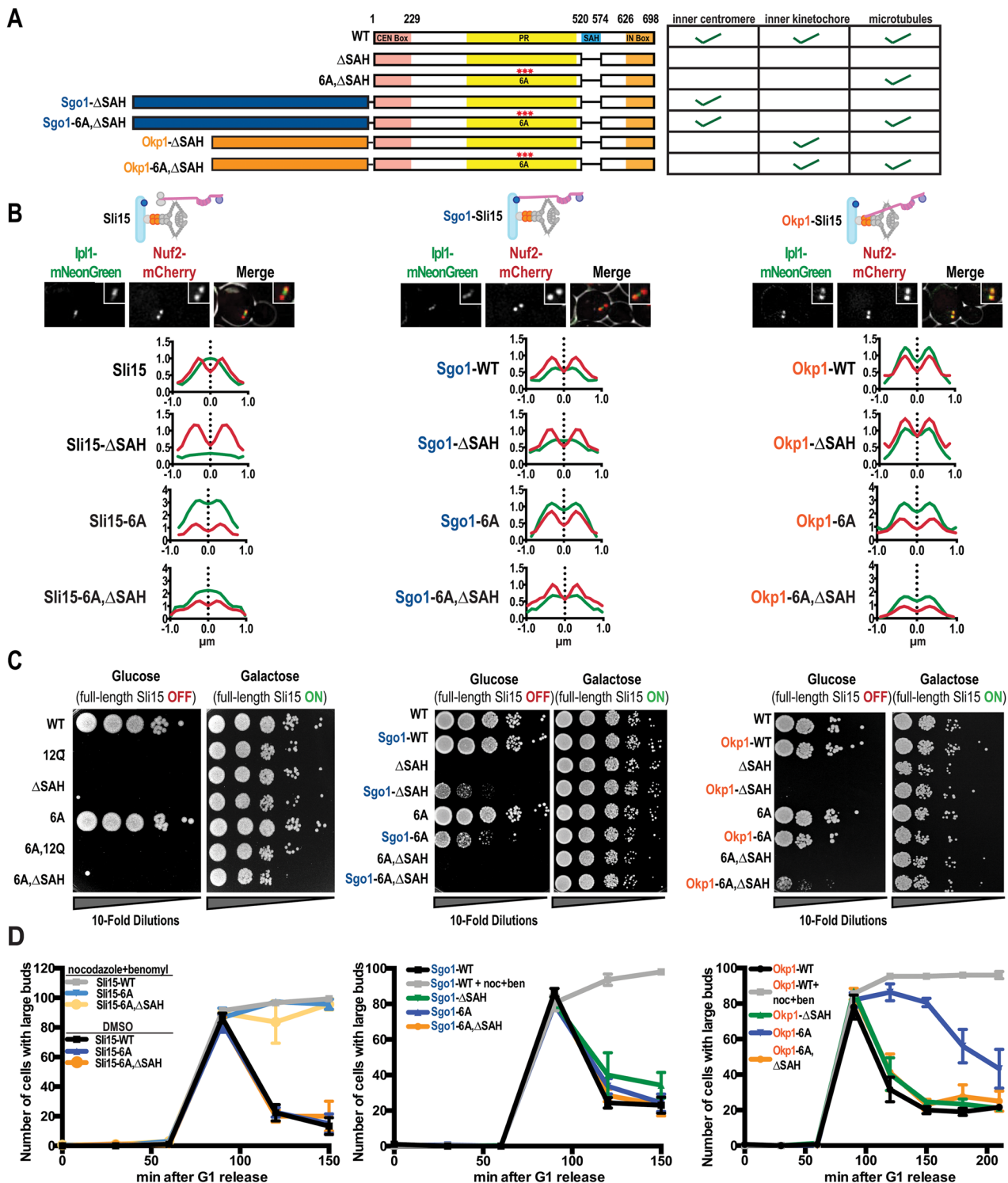


FIGURE 4: Inner centromere and inner kinetochore plus MTB constitute two independent CPC localization pathways. (A) Schematic of different Sli15 mutants and fusions to Sgo1 or Okp1. The table on the right shows the expected binding activities. (B) Line scan analysis along the spindle axis for the indicated Sli15 mutants and fusion constructs. CPC localization was monitored by measuring lpl1-mNeonGreen signal relative to Nuf2-mCherry. The intensities of mCherry and mNeonGreen signals of 20 cells were averaged and normalized to WT. Insert box for example images: 2.05 μm square. Note the different scales for the y axis in 6A, 6A,ΔSAH, Okp1-6A, and Okp1-6A,ΔSAH. (C) Tenfold serial dilution analysis of cells expressing the indicated Sli15 constructs with endogenous Sli15 under the control of a galactose inducible promoter. Dilutions were spotted on YPAD and YPAGR plates. (D) Budding index analysis of indicated Sli15 constructs. Cells were arrested in G1 and endogenous Sli15 was depleted. Fractions of large budded cells were determined every 30 min after release. The addition of nocodazole and benomyl (noc+ben) to Sli15-WT, Sgo1-WT or Okp1-WT was used as a positive control for metaphase arrest. Mean and SEM of three independent measurements are shown.

lead to chromosome biorientation (Supplemental Figure S3E). One explanation for increased chromosome missegregation could be that too much CPC activity results in continuous kinetochore–microtubule detachment. This would result in persistent activation of the SAC, which would lead to a metaphase arrest (Muñoz-Barrera and Monje-Casas, 2014). To test this hypothesis, we monitored cell growth as well as the cell cycle progression of cells released from G1. The Sli15-6A,ΔSAH construct did not rescue viability, nor affect cell cycle timing (Figure 4D and Supplemental Figure S3F) even when overexpressed (Supplemental Figure S3, G and H), indicating that the lethal phenotype results from too little CPC activity. When treated with nocodazole and benomyl, Sli15-6A,ΔSAH caused a metaphase arrest, indicating that this mutant did not impair the SAC (Figure 4D). We conclude that increased MTB by the CPC increases outer kinetochore phosphorylation globally without rescuing chromosome segregation. MTB activity of the CPC is therefore not sufficient for chromosome biorientation by the CPC.

How can the Sli15-6A,ΔSAH construct cause high levels of outer kinetochore phosphorylation without increasing chromosome biorientation? One possibility is that this mutant causes low rates of phosphorylation at all kinetochores, both misattached and bioriented. There are many phosphorylation sites for the CPC at the outer kinetochore, and phosphorylating only a few is unlikely to have much of an effect (Sarangapani *et al.*, 2013; Zaytsev *et al.*, 2015). To test if the Sli15-6A,ΔSAH lost its specificity to phosphorylate misattached kinetochores during chromosome biorientation, Ndc80 phosphorylation was monitored in cells over time from G1 to a Cdc20-depleted metaphase arrest (Supplemental Figure S4, A and B). Wild-type cells showed a strong accumulation of phosphorylation signal that peaked in preanaphase (60 min) and then disappeared again by the 180-min time point. A similar pattern was seen for cells with the Sli15-ΔSAH, only with lower overall levels of phosphorylation. Strikingly, Ndc80 phosphorylation levels continued to increase in Sli15-6A,ΔSAH expressing cells at time points when chromosome biorientation was already completed (Supplemental Figures S4A and S1D). Indeed, phosphorylation of Ndc80 by 6A,ΔSAH was even higher at the 180-min time point than at the 60-min time point. This suggests that it is incapable of specifically targeting misattached kinetochores. In agreement with this hypothesis, overexpression of Sli15-6A resulted in a metaphase arrest, indicating that it is capable of destabilizing the kinetochore–microtubule attachments of properly bioriented chromosomes leading to a continuous spindle checkpoint activation from unattached kinetochores (Supplemental Figure S3, G and H). This result is reminiscent of the continuous destabilization of attachments following the simultaneous overexpression of Sli15 and Ipl1 (Muñoz-Barrera and Monje-Casas, 2014). We conclude that the MTB activity of the CPC contributes to tension-independent outer kinetochore phosphorylation. However, at wild-type expression levels, the low levels of phosphorylation at each kinetochore are not sufficient for substantial destabilization of kinetochore–microtubule attachments.

MTB cooperates specifically with inner kinetochore binding to promote chromosome biorientation

These data suggest that CPC MTB generally promotes kinetochore phosphorylation, but additional binding activities are needed to target the kinase specifically to misattached kinetochores. To determine if either inner centromere or inner kinetochore targeting acts synergistically with MTB, we combined the 6A,ΔSAH mutant with the Sgo1 and Okp1 fusions. Surprisingly, increased MTB eliminated the rescue seen in the inner centromere-targeting Sgo1 fusion, suggesting incompatibility between the inner centromere and MTB

activities. For the combination of inner kinetochore (Okp1) targeting and MTB, this construct now partially rescued viability, restored chromosome segregation, and further increased Ndc80 phosphorylation (Figure 4C; Supplemental Figure S3, A and B). Since neither of these activities was able to rescue viability of the ΔSAH mutation on their own, this result demonstrates some form of cooperativity between inner kinetochore and MTB for CPC function (Figure 4C). Cooperativity between these two binding activities is also seen in the additive effect of Ndc80 phosphorylation by Okp1-6A,ΔSAH when compared with Okp1-ΔSAH or 6A,ΔSAH alone (Supplemental Figure S3B).

The opposing effects of MTB either complementing or conflicting with inner kinetochore versus inner centromere targeting were observed even in the absence of the ΔSAH mutation. Fusion of either the Okp1 or Sgo1 to the 6A mutation had a synthetic negative effect on growth (Figure 4C). However, the Okp1-fusion resulted in a strong metaphase delay, indicating that the combination of MTB with inner kinetochore binding results in too much CPC activity and the destabilization of properly bioriented kinetochore–microtubule attachments (Figure 4D). Deletion of the SAC protein Mad2 eliminated the observed metaphase delay, demonstrating that the Okp1-6A fusion construct generates an excess of unattached kinetochores (Supplemental Figure S5A). By contrast, the Sgo1-6A fusion did not cause a metaphase delay, suggesting that the combination of MTB with inner centromere binding results in too little activity and an increase in syntelic attachments (Figure 4D). The synthetic growth defect in Sgo1-6A mutants could be explained by the inability of these mutants to specifically enrich at the inner centromere (Supplemental Figure S5B). The opposing effects of MTB on inner centromere versus inner kinetochore localized CPC suggest that the inner centromere localization forms one pathway and the combined activities of the inner kinetochore and MTB form a second pathway. Consistent with this, combining Sgo1-ΔSAH with Okp1-6A,ΔSAH had an additive effect on growth when compared with the single fusion constructs (Supplemental Figure S5C).

To better understand the mechanism behind the synergistic effect of MTB and inner kinetochore binding, we tested whether inner kinetochore and MTB activities are required to be on the same molecule or whether they could rescue CPC function in *trans*. Simultaneous expression of constructs with microtubule targeting (Sli15-6A,ΔSAH) and inner kinetochore targeting (Okp1-ΔSAH) activities failed to rescue growth, unlike the construct with both targeting activities (Okp1-6A,ΔSAH, Supplemental Figure S5D). This indicates that microtubule and inner kinetochore binding of the CPC act synergistically in *cis*.

The results from the combination of *sli15-6A* with the fusion constructs suggest that MTB acts cooperatively with the inner kinetochore recruitment pathway, but not with the inner centromere recruitment pathway. We therefore hypothesized that increased CPC MTB would make the cells more reliant on Ctf19 and less dependent on Sgo1. To test this, we combined the *sli15-6A* mutation, which shows stronger spindle localization, with deletions of either Sgo1 or Ctf19 (Figure 5, A and B). By deleting *SGO1*, we forced the cells to use the inner kinetochore targeting pathway. The addition of the *sli15-6A* mutation resulted in a synthetic rescue phenotype, indicating that MTB promotes the activity of the inner kinetochore pathway. This effect became even more pronounced in the presence of moderate amounts of benomyl that sensitize the cells to chromosome segregation difficulties. Alternatively, deletion of *CTF19* would force the cells to use the inner centromere targeting pathway for chromosome biorientation. In this case, the addition of *sli15-6A* resulted in a synthetic growth defect, indicating that MTB acts

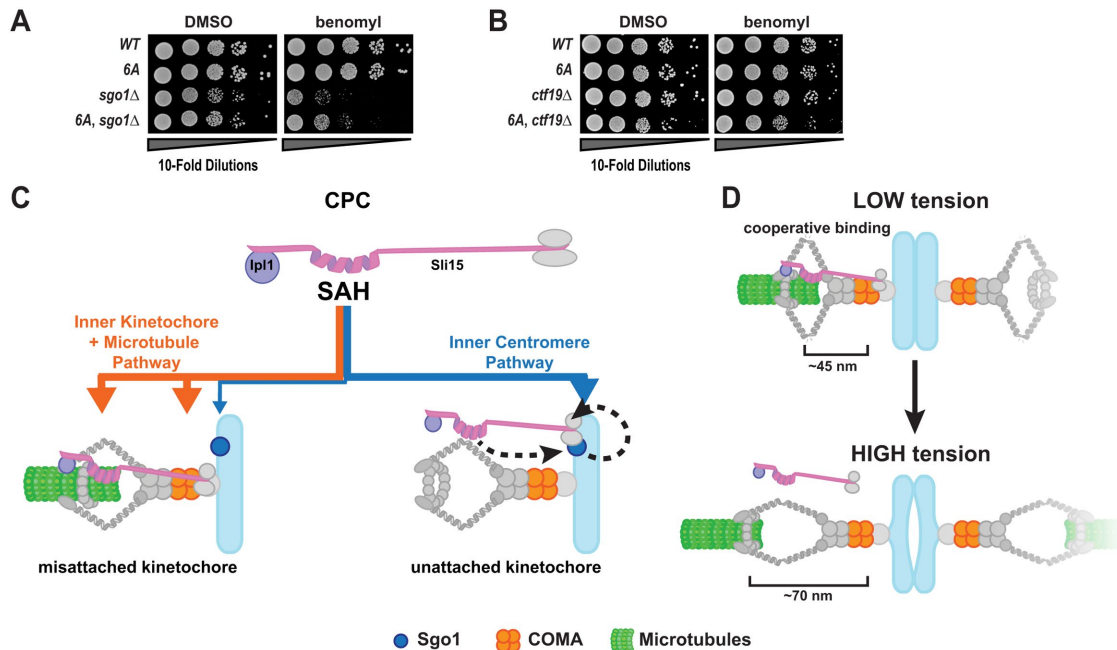


FIGURE 5: Two parallel pathways establish chromosome biorientation. (A and B) Tenfold serial dilution of the indicated genotypes. Cells were spotted on YPAD plates containing DMSO or benomyl (10 $\mu\text{g}/\text{ml}$). (C) Model for how CPC binding activities contribute to chromosome biorientation. The SAH contributes to binding to microtubules (green), inner kinetochore (orange), and inner centromere (blue). Inner centromere localization is regulated by a positive feedback loop between the CPC and Sgo1. The inner centromere targeting forms one pathway primarily acting on unattached kinetochores, while the inner kinetochore and MTB act cooperatively to form a second pathway primarily acting on misattached kinetochores. (D) Potential mechanism for how the CPC localizes specifically to misattached kinetochores. At misattached kinetochores, one Sli15 molecule can bind simultaneously to the inner kinetochore and a microtubule. At bioriented kinetochores that are under tension, the increased distance between the inner kinetochore and the microtubules would prevent cooperative binding. Intrakinetochores distances are based on previously published measurements (Joglekar *et al.*, 2009).

antagonistically to the inner centromere pathway. Taken together, the data indicate that the CPC acts via two different localization pathways, one via inner centromere binding and one via inner kinetochore plus MTB.

DISCUSSION

To ensure faithful chromosome segregation, the CPC localizes to the inner centromere, the inner kinetochore and microtubules. These localizations contribute to different CPC functions, as inner centromere localization has been linked to cohesion maintenance and SAC silencing in human cells, whereas inner kinetochore binding of the CPC has been shown to promote SAC signaling and outer kinetochore assembly in *Xenopus* egg extracts (Hengeveld *et al.*, 2017; Bonner *et al.*, 2019). In addition, SAH MTB activity has been shown to contribute to outer kinetochore phosphorylation and SAC activation in human cells (Wheelock *et al.*, 2017).

Previous work in budding yeast has demonstrated that either inner centromere or inner kinetochore targeting of the CPC is necessary for biorientation, indicating that these binding activities are each required for two redundant pathways (Fischböck-Halwachs *et al.*, 2019; García-Rodríguez *et al.*, 2019). Here we set out to determine how the third known binding activity of the CPC, to microtubules, contributes to chromosome biorientation. After disrupting the MTB SAH domain with either deletions or amino acid substitutions, we were surprised to observe a complete lack of clear localization for the CPC during the time at which chromosome biorientation takes place. Moreover, these SAH mutants are lethal, have reduced chromosome biorientation, missegregate chromosomes

at extremely high rates, and fail to phosphorylate the kinetochore substrates Ndc80 and Dam1. In agreement with these results, SAH deletion in human cell culture decreases kinetochore phosphorylation and mitotic checkpoint activity (Vader *et al.*, 2007; Wheelock *et al.*, 2017). We conclude that the SAH domain is essential for accurate chromosome biorientation because it contributes to the localization of CPC to the inner centromere, inner kinetochore, and microtubules.

To determine the relative contribution of each of these activities, we disrupted these three pathways through depletion of Sgo1 (inner centromere), deletion of Ctf19 (inner kinetochore), or depolymerization of microtubules. In the presence of microtubules, perturbation of the Sgo1 and Ctf19 pathways showed similar decreases in CPC localization. However, after microtubule depolymerization, only the Sgo1 pathway contributed measurably to CPC localization. This observation is consistent with the known mechanism of Sgo1 recruitment to the inner centromere. Unattached kinetochores bind the kinase Mps1, which phosphorylates Knl1/Spc105 on conserved repeats of the MELT motif (London *et al.*, 2012; Shepperd *et al.*, 2012; Yamagishi *et al.*, 2012; Vleugel *et al.*, 2015). Phosphorylated MELT repeats bind the kinase Bub1. Knl1-bound Bub1 can activate both the SAC and the phosphorylate Histone H2A on Serine 121 (Meraldi and Sorger, 2005; Kawashima *et al.*, 2010). Phosphorylation of H2A greatly increases its affinity for Sgo1 (Kawashima *et al.*, 2010; Ricke *et al.*, 2012). In human cells, haspin-mediated phosphorylation of histone H3 at Thr3 provides an additional centromeric recruitment pathway of the CPC (Kelly *et al.*, 2010; Wang *et al.*, 2010; Yamagishi *et al.*, 2010). However, deletion of the haspin-like genes

ALK1 and *ALK2* in budding yeast has no impact on growth, indicating that this pathway is not active in yeast (Campbell and Desai, 2013). We conclude that this inner centromeric CPC recruitment can occur independently of microtubules. This recruitment to unattached kinetochores may contribute to the CPC's role in maintaining the SAC by preventing PP1 phosphatase binding to Knl1/Spc105 (Liu *et al.*, 2010; Rosenberg *et al.*, 2011). In contrast with the inner centromere binding, we find that the inner kinetochore binding relies on the presence of microtubules. These results demonstrate that the two pathways are recruited differentially to distinctive kinetochore–microtubule attachment states, as the inner centromeric recruitment pathway is primarily used at unattached kinetochores (Figure 5C).

Two studies have recently demonstrated that the inner centromere and inner kinetochore recruitment pathways are partially redundant for biorientation, and disruption of both pathways simultaneously is lethal (Fischböck-Halwachs *et al.*, 2019; García-Rodríguez *et al.*, 2019). Both studies demonstrated that ectopic targeting of Sli15 to the inner kinetochore rescues chromosome biorientation under these conditions. However, it was not known if either of these binding activities is sufficient for the process or if they additionally require MTB. The lack of any observable CPC localization in the SAH deletion allowed us to use this mutant to then restore the targeting to specific regions and determine how each of the known CPC interactions contributes to chromosome biorientation and kinetochore phosphorylation. We found that targeting the CPC to the inner centromere was partially sufficient to restore viability in the SAH mutants independently of the other localization activities. We did not find any evidence of cooperativity between the inner centromere and the microtubule targeting pathways. Sgo1-based recruitment of the CPC was robust even in the absence of microtubules. This is in agreement with results in human cells that show robust inner centromere localization after nocodazole treatment (Wang *et al.*, 2011; Matson and Stukenberg, 2014; Hadders *et al.*, 2020). Furthermore, when we forced cells to use the inner centromere-targeting pathway either through the Sgo1- Δ SAH construct or by deleting Ctf19, increased Sli15 MTB resulted in decreased viability. We conclude that the inner centromere targeting pathway functions independently of, and may even be antagonistic to, MTB activity.

Restoration of either inner kinetochore or MTB activity to Sli15- Δ SAH individually was not sufficient to rescue biorientation. However, the combination of the two partially rescued cell viability and chromosome segregation, suggesting that they act cooperatively. In addition, when we forced cells to biorient via the inner kinetochore pathway by deleting Sgo1, increased MTB improved growth. Finally, we do not observe any contribution of Ctf19 to CPC localization in the absence of microtubules. These three lines of evidence lead us to conclude that the inner kinetochore and MTB activities of Sli15 act cooperatively (Figure 5C). We find that both activities need to be present on the same molecule, as they cannot rescue in *trans*. Intriguingly, MTB alone leads to outer kinetochore phosphorylation in metaphase arrested cells with intact spindles, which strongly suggests a tension-independent targeting of kinase activity to attached kinetochores. Recently published results for a Borealin-based MTB activity suggest that a similar mechanism occurs in human cells (Trivedi *et al.*, 2019). However, the MTB activity is not sufficient for chromosome biorientation, indicating that inner kinetochore binding imparts a necessary specificity for misattached kinetochores to this pathway.

The cooperativity between microtubule and inner kinetochore binding on the same molecule provides for a simple mechanism to direct the CPC specifically to misattached kinetochores (Figure 5D).

Under this model, the CPC only directly interacts with kinetochores where it can simultaneously bind to the inner kinetochore and microtubules, presumably due to low binding affinities to each of these sites individually. Therefore the CPC would not bind directly to the inner kinetochores of unattached kinetochores because of the lack of microtubules, as we observed via a lack of Ctf19 contribution to CPC localization at unattached kinetochores. The complex would also have a decreased affinity for bioriented attachments, as the increased tension would greater the distance between the inner kinetochore and the microtubules such that both could not be bound by the same molecule at the same time. This mechanism is similar to the “dog-leash” model proposed for a tension-dependent increase in the distance between the CPC bound to the inner centromere and its substrates at the outer kinetochore (Santaguida and Musacchio, 2009). However, one key difference is that in our model, tension would decrease the affinity between the CPC and the kinetochore–microtubule interface. In agreement with this model, localization of the CPC to the kinetochore is decreased during chromosome biorientation as measured by immunofluorescence with phosphospecific antibodies in human cells (DeLuca *et al.*, 2011; Broad *et al.*, 2020). Alternatively, the MTB activity of the SAH could orient the IN box of inner kinetochore-bound Sli15 toward the outer kinetochore.

In summary, we show that the SAH domain of Sli15 contributes to all known CPC localizations during error correction. By analyzing the contributions of each localization to CPC function, we determined that two CPC localization pathways are partially sufficient for viability, one acting at the inner centromere and one at the inner kinetochore plus microtubules. Furthermore, our data suggest that the inner centromere pathway acts primarily on unattached kinetochores, whereas the inner kinetochore plus MTB acts on misattached kinetochores.

MATERIALS AND METHODS

[Request a protocol](#) through *Bio-protocol*.

Yeast strains and media

All yeast strains used were grown in yeast extract/peptone containing 40 μ g/ml adenine-HCl (YPA) and 2% glucose (YPAD) or 1% raffinose and 1% galactose (YPAGR). Unless otherwise stated, cultures were grown at 30°C. Serial dilutions were grown for 2 d at 30°C. Galactose inducible promoters, fluorescent tags, epitope tags, and gene deletions were introduced into the genomic loci as previously described (Longtine *et al.*, 1998). Sli15 constructs were cloned into plasmids via Gibson assembly (Gibson *et al.*, 2009). Plasmids were integrated at the URA3 or TRP1 loci by digesting the plasmids with *Bst*BI or *Bsg*I, respectively. All integrations and plasmids were checked by sanger sequencing.

Yeast transformation

PCR products or digested plasmids were transformed into cells pelleted from 50 ml exponentially growing cultures. Cells were washed once with TE (10 mM Tris, pH 7.5, and 1 mM EDTA) and once with LiAc/TE (100 mM LiAc, 10 mM Tris, pH 7.5, and 1 mM EDTA). Cells were resuspended in LiAc/TE and 100 μ l were added to 10 μ l plasmid or PCR product, 10 μ l single-stranded sheared salmon sperm DNA, and 750 μ l PEG/LiAc/TE (40% PEG 4000, 100 mM LiAc, 10 mM Tris, and 1 mM EDTA, pH 7.5). After 30 min at 30°C, 80 μ l DMSO were added and incubated at 42°C for 15 min. The cells were pelleted, resuspended in SOS (0.3 YPAD or YPAGR and 6 mM CaCl₂), plated on selective plates, and incubated for 2 d at 30°C.

Yeast synchronization and galactose inducible depletion

To deplete proteins under the control of a *Gal10-1* promoter, cells were synchronized for 45 min in YPAGR containing α -factor (10 μ g/ml). Media were exchanged with YPAD containing α -factor and grown for an additional 2 h and 15 min. Cells were then released into the cell cycle by washing twice with YPAD and adding Pronase E (Merck). For Pds1 degradation, cells were washed once with YPAD 30 min after release and α -factor (10 μ g/ml) was added again every 30 min. For the M-track assay in Figure 1G, rapamycin was added 20 min after G1 release after which cells were arrested in metaphase for an additional 80 min by depletion of Cdc20. Nocodazole (VWR) was used at a concentration of 10 μ M and benomyl (Sigma-Aldrich) was used at 68 μ M. Rapamycin (Santa Cruz Biotechnology) was used at a concentration of 1 μ M.

Protein extraction and Western blotting

For yeast protein extraction, saturated overnight cultures were diluted into 5 ml YPAGR to an OD of 0.25. After synchronization and depletion of Sli15 and/or Cdc20, cells were released into the cell cycle and, unless otherwise stated, harvested 60 min after release. Proteins were extracted by pelleting the cells, resuspending in 100 μ l trichloroacetic acid (5%), and incubating them for 10 min at room temperature. Cells were washed once with 1 ml ddH₂O and resuspended in 100 μ l lysis buffer (50 mM Tris, pH 7.4, 50 mM dithiothreitol (DTT), 1 mM EDTA, cOmplete EDTA-free protease inhibitor cocktail [Roche] and Phosstop [Roche]). Glass beads were added and the cells were vortexed for 30 min at 4°C. Unless otherwise stated, M-track samples were resuspended in lysis buffer without Phosstop. To test the specificity of the trimethylation antibody, calf intestinal phosphatase (Quick CIP, New England Biolabs) for 1 h at 37°C; 33 μ l 4 \times sample buffer were added and incubated at 95°C for 3 min. The samples were stored at -20°C. To measure Sli15 expression, cells were harvested, pelleted, and resuspended in 100 μ l NaOH (0.2 M); pelleted and resuspended in 1 \times sample buffer before incubating them at 95°C for 3 min; and stored at -20°C. For immunoblots, the following antibodies were used: mouse anti-Pgk1 monoclonal 22C5D8 (Thermo Fisher Scientific), rat anti-HA-clone 3F10 (Roche), mouse anti-Myc monoclonal 4A6 (EMD Millipore), rabbit anti-p-Histone H3 (Ser 10) polyclonal (Santa Cruz Biotechnology), mouse anti-maltose binding protein monoclonal antibody IgG2a (New England Biolabs), mouse anti-Histone H3 [Trimethyl Lys9] 6F12-H4 [Novus Biologicals], and rabbit anti-Ndc80 phospho-S37 polyclonal. Phosphospecific antibodies were used with 40 μ M unphosphorylated competitor peptide. Membranes were then probed with the corresponding secondary antibodies: anti-rat IgG-HRP-linked (Cell Signaling Technology), anti-rabbit IgG-HRP-linked (Cell Signaling Technology), or anti-mouse IgG-HRP-linked (Cell Signaling Technology). Immunoblots were quantified using ImageJ (National Institutes of Health).

Microscopy

Unless otherwise stated, cells were synchronized as described above and imaged 60 or 90 min after release. Cells were pelleted and washed twice with 1 ml sterile ddH₂O and resuspended in 100 μ l sterile ddH₂O, and 2 μ l of cell suspension were spotted onto 1% agarose pads supplemented with complete synthetic media and 2% glucose. A coverslip was placed on top and sealed with VALAP (1:1:1 mixture by weight of paraffin [Merk], lanolin [Alfa Aesar], and Vaseline [Ferd. Eimermacher]). Images were collected on a Delta-Vision Ultra Epifluorescence Microscope system (Cytiva) at 23°C and a PlanApo N 60/1.42 Oil objective and a sCMOS sensor, 6.5 μ m pixel size camera; 12 z sections with a step size of 0.5 μ m were

taken, except for the chromosome missegregation assay where 24 z sections were taken. For the chromosome biorientation assay, images were collected 60 and 180 min after G1 release performing a time-lapse series for 4 min at 15-s intervals. Images were deconvolved using softWoRx software (Life Sciences Software). Quantifications and subsequent normalizations were performed from images obtained on the same day and representative images were contrast adjusted identically using ImageJ. For spindle localization in pre-anaphase and anaphase cells, ImageJ was used to measure the intensity distribution of a perpendicular line (5 pixels wide) to the spindle center. The obtained intensities were fitted to a Gaussian curve and subsequently integrated as previously described (Fink et al., 2017). For this analysis, nondeconvolved images were used. For line-scan analysis intensity distributions of a line (5 pixels wide) along the spindle axis were background subtracted and the average of 20 cells was calculated. For CPC localization in nocodazole and benomyl (Figure 3A) intensities of mCherry and mNeonGreen signals were measured by first drawing a circle around mCherry signals and obtaining the mNeonGreen intensities from the same circle in the mNeonGreen channel. Background was subtracted from the surrounding area in the respective channel.

Recombinant protein expression and purification

Sli15 MTB domain constructs were designed with an MBP (maltose binding protein) tag at the N terminus and a 6 \times Histidine tag at the C terminus. All proteins were expressed in *E. coli* Rosetta pLysS. Overnight cultures were each inoculated in 2 l of 2XTY medium containing 50 μ g/ml kanamycin and grown at 37°C to OD 600 of 1. Protein expression was induced at 18°C by 0.3 mM IPTG for 15 h. Harvested cells were resuspended in lysis buffer (50 mM Tris, pH 7.4, 300 mM KCl, 10% Glycerol, 1 mM DTT) containing one cOmplete Mini EDTA free protease inhibitor cocktail tablet and 0.2 mM PMSF and lysed by sonication. Lysates were centrifuged at 14,000 rpm at 4°C and the supernatants clarified with a 0.2- μ m membrane syringe filter (VWR International) before proceeding with a two-step purification protocol. Clarified lysates were passed on pre-equilibrated Histrap HP columns (GE Healthcare). The columns were washed with wash buffer (lysis buffer with 40 mM Imidazole) and the bound proteins were eluted in incremental fractions with 100, 150, and 200 mM imidazole. Pooled eluted fractions were concentrated with Ultracel-30 (Millipore) and injected on pre-equilibrated Superdex Hi-Load S200 16/60 or 26/600 (GE Healthcare) at 4°C with lysis buffer. Protein fractions were collected and frozen in liquid nitrogen and stored at -80°C.

Microtubule pelleting assay

Porcine brain tubulin (Cytoskeleton, Inc) reconstituted with tubulin buffer (80 mM PIPES, pH 6.9, 1 mM MgCl₂, 0.5 mM EGTA, supplemented with GTP) was thawed and spun in an ultracentrifuge (Beckman Coulter OptimaMax) at 70k rpm for 5 min, 4°C to remove insoluble protein. To polymerize tubulin, 1 mM GTP was added, and 1 and 10 μ M taxol were sequentially added and incubated at 37°C for 10 min each. After incubation at 37°C for another 15 min, the microtubules were added to a 40% glycerol cushion containing tubulin buffer, GTP, and taxol and spun in an ultracentrifuge at 37°C for 20 min. The pellet was rinsed with water and resuspended in tubulin buffer with 20 μ M taxol to yield 10 μ M polymerized microtubules.

For pelleting assays, recombinant MBP fusion proteins purified from *E. coli* were thawed from -80°C and first spun at 70k rpm for 30 min at 4°C in an ultracentrifuge. Supernatants were carefully separated and diluted in buffer containing 50 mM Tris, pH 7.4,

150 mM KCl, 10% glycerol, and 1 mM DTT. 25 nM protein was added to 1 μ M taxol-stabilized microtubules in 50 μ l reactions and incubated for 10 min at 25°C. All reactions contained 0.2 mg/ml bovine serum albumin. Pellets and supernatants were separated by ultracentrifugation as above at 25°C and heated with SDS sample buffer at 95°C for 5 min.

Statistical analysis

Statistical significance between samples was assessed via one-way ANOVA analysis with uncorrected Fisher's LSD using Prism 6 (Graphpad).

Computer code and code availability

The Python script used in Figures 2E and 4B to determine the localization of the CPC relative to Nuf2 was developed for this study. Briefly, from deconvolved images, a line (5 pixels wide) along the Nuf2-mCherry signals was drawn and fluorescence signal intensities along this line were obtained for mCherry and mNeonGreen. After background subtraction, a signal intensity threshold of the mCherry signal defined the length of the spindle. The obtained position and corresponding intensity values for mCherry and mNeonGreen were averaged for all spindles analyzed from the same sample. Normalization to WT and data plotting were performed in Excel (Microsoft) and Prism 6 (Graphpad), respectively. The code is available by the authors on request.

ACKNOWLEDGMENTS

The authors thank the Campbell and Dammermann laboratories as well as Franz Klein for helpful discussions and comments on the paper. We thank Peter Schlögelhofer, Franz Klein, and Gustav Ammerer for gifts of yeast strains and plasmids. We thank Ana Markovic for helping set up the M-track assay. We acknowledge the service of the Perutz Labs Central Biooptics-Light Microscopy, a member of VLSI. This work was supported by Vienna Science and Technology Fund (WWTF) Grant VRG14-001 and Austrian Science Fund (FWF) Grants Y944-B28 and W1238-B20 to C.S.C.

REFERENCES

Ainsztein AM, Kandels-Lewis SE, Mackay AM, Earnshaw WC (1998). INCENP centromere and spindle targeting: identification of essential conserved motifs and involvement of heterochromatin protein HP1. *J Cell Biol* 143, 1763–1774.

Biggins S, Severin FF, Bhalla N, Sassoon I, Hyman AA, Murray AW (1999). The conserved protein kinase Ipl1 regulates microtubule binding to kinetochores in budding yeast. *Genes Dev* 13, 532–544.

Bonner MK, Haase J, Swiderman J, Halas H, Miller Jenkins LM, Kelly AE (2019). Enrichment of Aurora B kinase at the inner kinetochore controls outer kinetochore assembly. *J Cell Biol* 218, 3237–3257.

Boyarchuk Y, Salic A, Dasso M, Arnaoutov A (2007). Bub1 is essential for assembly of the functional inner centromere. *J Cell Biol* 176, 919–928.

Brezovich A, Schuschnig M, Ammerer G, Kraft C (2015). An in vivo detection system for transient and low-abundant protein interactions and their kinetics in budding yeast. *Yeast* 32, 355–365.

Broad AJ, DeLuca JG (2020). The right place at the right time: Aurora B kinase localization to centromeres and kinetochores. *Essays Biochem* doi:10.1042/EBC20190081.

Broad AJ, DeLuca KF, DeLuca JG (2020). Aurora B kinase is recruited to multiple discrete kinetochore and centromere regions in human cells. *J Cell Biol* 219. doi:10.1083/jcb.201905144.

Campbell CS, Desai A (2013). Tension sensing by Aurora B kinase is independent of survivin-based centromere localization. *Nature* 497, 118 EP-121.

Cheeseman IM, Chappie JS, Wilson-Kubalek EM, Desai A (2006). The conserved KMN network constitutes the core microtubule-binding site of the kinetochore. *Cell* 127, 983–997.

Cheeseman IM, Anderson S, Jwa M, Green EM, Kang JS, Yates JR, Chan CSM, Drubin DG, Barnes G (2002). Phospho-regulation of kinetochore-microtubule attachments by the Aurora kinase Ipl1p. *Cell* 111, 163–172.

Cimini D, Wan X, Hirel CB, Salmon ED (2006). Aurora kinase promotes turnover of kinetochore microtubules to reduce chromosome segregation errors. *Curr Biol* 16, 1711–1718.

Dai J, Sullivan BA, Higgins JMG (2006). Regulation of mitotic chromosome cohesion by Haspin and Aurora B. *Dev Cell* 11, 741–750.

DeLuca JG, Gall WE, Ciferri C, Cimini D, Musacchio A, Salmon ED (2006). Kinetochore microtubule dynamics and attachment stability are regulated by Hec1. *Cell* 127, 969–982.

DeLuca KF, Lens SMA, DeLuca JG (2011). Temporal changes in Hec1 phosphorylation control kinetochore-microtubule attachment stability during mitosis. *J Cell Sci* 124, 622–634.

Fink S, Turnbull K, Desai A, Campbell CS (2017). An engineered minimal chromosomal passenger complex reveals a role for INCENP/Sli15 spindle association in chromosome biorientation. *J Cell Biol* 216, 911–923.

Fischböck-Halwachs J, Singh S, Potocnjak M, Hagemann G, Solis-Mezarino V, Woike S, Ghodgaonkar-Steger M, Weissmann F, Gallego LD, Rojas J, et al. (2019). The COMA complex interacts with Cse4 and positions Sli15/Ipl1 at the budding yeast inner kinetochore. *elife* 8. doi:10.7554/eLife.42879.

Funabiki H (2019). Correcting aberrant kinetochore microtubule attachments: a hidden regulation of Aurora B on microtubules. *Curr Opin Cell Biol* 58, 34–41.

García-Rodríguez LJ, Kasčiukovic T, Denninger V, Tanaka TU (2019). Aurora B-INCENP Localization at Centromeres/Inner Kinetochores Is Required for Chromosome Bi-orientation in Budding Yeast. *Curr Biol* 29, 1536–1544.e4.

Gibson DG, Young L, Chuang R-Y, Venter JC, Hutchison CA, Smith HO (2009). Enzymatic assembly of DNA molecules up to several hundred kilobases. *Nat. Methods* 6, 343–345.

Gillett ES, Espelin CW, Sorger PK (2004). Spindle checkpoint proteins and chromosome-microtubule attachment in budding yeast. *J Cell Biol* 164, 535–546.

Hadders MA, Hindriksen S, Truong MA, Mhaskar AN, Wopken JP, Vromans MJM, Lens SMA (2020). Untangling the contribution of Haspin and Bub1 to Aurora B function during mitosis. *J Cell Biol* 219, 253.

Hengeveld RCC, Vromans MJM, Vleugel M, Hadders MA, Lens SMA (2017). Inner centromere localization of the CPC maintains centromere cohesion and allows mitotic checkpoint silencing. *Nat Commun* 8, 15542.

Jin QW, Fuchs J, Loidl J (2000). Centromere clustering is a major determinant of yeast interphase nuclear organization. *J Cell Sci* 113(Pt 11), 1903–1912.

Joglekar AP, Bloom K, Salmon ED (2009). In vivo protein architecture of the eukaryotic kinetochore with nanometer scale accuracy. *Curr Biol* 19, 694–699.

Kang J, Cheeseman IM, Kallstrom G, Velmurugan S, Barnes G, Chan CS (2001). Functional cooperation of Dam1, Ipl1, and the inner centromere protein (INCENP)-related protein Sli15 during chromosome segregation. *J Cell Biol* 155, 763–774.

Kawashima SA, Yamagishi Y, Honda T, Ishiguro K-I, Watanabe Y (2010). Phosphorylation of H2A by Bub1 prevents chromosomal instability through localizing shugoshin. *Science* 327, 172–177.

Keating P, Rachidi N, Tanaka TU, Stark MJR (2009). Ipl1-dependent phosphorylation of Dam1 is reduced by tension applied on kinetochores. *J Cell Sci* 122, 4375–4382.

Kelly AE, Ghenoiu C, Xue JZ, Zierhut C, Kimura H, Funabiki H (2010). Survivin reads phosphorylated histone H3 threonine 3 to activate the mitotic kinase Aurora B. *Science* 330, 235–239.

Klein UR, Nigg EA, Gruneberg U (2006). Centromere targeting of the chromosomal passenger complex requires a ternary subcomplex of Borealin, Survivin, and the N-terminal domain of INCENP. *Mol Biol Cell* 17, 2547–2558.

Knowlton AL, Lan W, Stukenberg PT (2006). Aurora B is enriched at merotelic attachment sites, where it regulates MCAK. *Curr Biol* 16, 1705–1710.

Krenn V, Musacchio A (2015). The Aurora B Kinase in Chromosome Bi-Oriented and Spindle Checkpoint Signaling. *Front Oncol* 5, 225.

Lampson MA, Cheeseman IM (2011). Sensing centromere tension: Aurora B and the regulation of kinetochore function. *Trends Cell Biol* 21, 133–140.

Lampson MA, Renduchitala K, Khodjakov A, Kapoor TM (2004). Correcting improper chromosome-spindle attachments during cell division. *Nat Cell Biol* 6, 232–237.

Liu D, Vleugel M, Backer CB, Hori T, Fukagawa T, Cheeseman IM, Lampson MA (2010). Regulated targeting of protein phosphatase 1 to the outer kinetochore by KNL1 opposes Aurora B kinase. *J Cell Biol* 188, 809–820.

- London N, Ceto S, Ranish JA, Biggins S (2012). Phosphoregulation of Spc105 by Mps1 and PP1 Regulates Bub1 Localization to Kinetochores. *Curr Biol*. doi:10.1016/j.cub.2012.03.052.
- Longtine MS, McKenzie A, Demarini DJ, Shah NG, Wach A, Brachat A, Philippsen P, Pringle JR (1998). Additional modules for versatile and economical PCR-based gene deletion and modification in *Saccharomyces cerevisiae*. *Yeast* 14, 953–961.
- Makrantonis V, Stark MJR (2009). Efficient chromosome biorientation and the tension checkpoint in *Saccharomyces cerevisiae* both require Bir1. *Mol Cell Biol* 29, 4552–4562.
- Matson DR, Stukenberg PT (2014). CENP-I and Aurora B act as a molecular switch that ties RZZ/Mad1 recruitment to kinetochore attachment status. *J Cell Biol* 205, 541–554.
- Meraldi P, Sorger PK (2005). A dual role for Bub1 in the spindle checkpoint and chromosome congression. *EMBO J* 24, 1621–1633.
- Mirchenko L, Uhlmann F (2010). Sli15(INCENP) dephosphorylation prevents mitotic checkpoint reengagement due to loss of tension at anaphase onset. *Curr Biol* 20, 1396–1401.
- Muñoz-Barrera M, Monje-Casas F (2014). Increased Aurora B activity causes continuous disruption of kinetochore–microtubule attachments and spindle instability. *Proc Natl Acad Sci USA* doi:10.1073/pnas.1408017111.
- Nerushcheva OO, Galander S, Fernius J, Kelly D, Marston AL (2014). Tension-dependent removal of pericentromeric shugoshin is an indicator of sister chromosome biorientation. *Genes Dev* 28, 1291–1309.
- Peckham M, Knight PJ (2009). When a predicted coiled coil is really a single α -helix, in myosins and other proteins - Soft Matter (RSC Publishing). *Soft Matter*, DOI:10.1039/B822339D.
- Pereira G (2003). Separase Regulates INCENP-Aurora B Anaphase Spindle Function Through Cdc14. *Science* 302, 2120–2124.
- Ravichandran MC, Fink S, Clarke MN, Hofer FC, Campbell CS (2018). Genetic interactions between specific chromosome copy number alterations dictate complex aneuploidy patterns. *Genes Dev* 32, 1485–1498.
- Resnick TD, Satinover DL, Maclsaac F, Stukenberg PT, Earnshaw WC, Orr-Weaver TL, Carmena M (2006). INCENP and Aurora B promote meiotic sister chromatid cohesion through localization of the Shugoshin MEI-S332 in *Drosophila*. *Dev Cell* 11, 57–68.
- Ricke RM, Jegathanan KB, Malureanu L, Harrison AM, van Deursen JM (2012). Bub1 kinase activity drives error correction and mitotic checkpoint control but not tumor suppression. *J Cell Biol* 199, 931–949.
- Rosenberg JS, Cross FR, Funabiki H (2011). KNL1/Spc105 recruits PP1 to silence the spindle assembly checkpoint. *Curr Biol* 21, 942–947.
- Salimian KJ, Ballister ER, Smoak EM, Wood S, Panchenko T, Lampson MA, Black BE (2011). Feedback control in sensing chromosome biorientation by the Aurora B kinase. *Curr Biol* 21, 1158–1165.
- Samejima K, Platani M, Wolny M, Ogawa H, Vargiu G, Knight PJ, Peckham M, Earnshaw WC (2015). The inner centromere protein (INCENP) coil is a single α -helix (SAH) domain that binds directly to microtubules and is important for chromosome passenger complex (CPC) localization and function in mitosis. *J Biol Chem* 290, 21460–21472.
- Santaguida S, Musacchio A (2009). The life and miracles of kinetochores. *EMBO J* 28, 2511–2531.
- Sarangapani KK, Akiyoshi B, Duggan NM, Biggins S, Asbury CL (2013). Phosphoregulation promotes release of kinetochores from dynamic microtubules via multiple mechanisms. *Proc Natl Acad Sci USA* 110, 7282–7287.
- Shepherd LA, Meadows JC, Sochaj AM, Lancaster TC, Zou J, Buttrick GJ, Rappilber J, Hardwick KG, Millar JBA (2012). Phosphodependent recruitment of Bub1 and Bub3 to Spc7/KNL1 by Mph1 kinase maintains the spindle checkpoint. *Curr Biol* doi:10.1016/j.cub.2012.03.051.
- Storchova Z, Becker JS, Talarek N, Kögelsberger S, Pellman D (2011). Bub1, Sgo1, and Mps1 mediate a distinct pathway for chromosome biorientation in budding yeast. *Mol Biol Cell* 22, 1473–1485.
- Tanaka TU, Rachidi N, Janke C, Pereira G, Galova M, Schiebel E, Stark MJR, Nasmyth K (2002). Evidence that the Ipl1-Sli15 (Aurora kinase-INCENP) complex promotes chromosome bi-orientation by altering kinetochore-spindle pole connections. *Cell* 108, 317–329.
- Trivedi P, Zaytsev AV, Godzi M, Ataullakhanov FI, Grishchuk EL, Stukenberg PT (2019). The binding of Borealin to microtubules underlies a tension independent kinetochore–microtubule error correction pathway. *Nat Commun* 10, 1–19.
- Tseng BS, Tan L, Kapoor TM, Funabiki H (2010). Dual detection of chromosomes and microtubules by the chromosomal passenger complex drives spindle assembly. *Dev Cell* 18, 903–912.
- Vader G, Crujisen CWA, van Harn T, Vromans MJM, Medema RH, Lens SMA (2007). The chromosomal passenger complex controls spindle checkpoint function independent from its role in correcting microtubule kinetochore interactions. *Mol Biol Cell* 18, 4553–4564.
- van der Horst A, Lens SMA (2013). Cell division: control of the chromosomal passenger complex in time and space. *Chromosoma* doi:10.1007/s00412-013-0437-6.
- van der Horst A, Vromans MJM, Bouwman K, van der Waal MS, Hadders MA, Lens SMA (2015). Inter-domain cooperation in INCENP promotes aurora B relocation from centromeres to microtubules. *Cell Rep* 12, 380–387.
- van der Waal MS, Saurin AT, Vromans MJM, Vleugel M, Wurzenberger C, Gerlich DW, Medema RH, Kops GJPL, Lens SMA (2012). Mps1 promotes rapid centromere accumulation of Aurora B. *EMBO Rep* doi:10.1038/embor.2012.93.
- Verzijlbergen KF, Nerushcheva OO, Kelly D, Kerr A, Clift D, de Lima Alves F, Rappilber J, Marston AL (2014). Shugoshin biases chromosomes for biorientation through condensin recruitment to the pericentromere. *elife* 3, e01374.
- Vleugel M, Omerzu M, Groenewold V, Hadders MA, Lens SMA, Kops GJPL (2015). Sequential multisite phospho-regulation of KNL1-BUB3 interfaces at mitotic kinetochores. *Mol Cell* 57, 824–835.
- Waizenegger IC, Hauf S, Meinke A, Peters JM (2000). Two distinct pathways remove mammalian cohesin from chromosome arms in prophase and from centromeres in anaphase. *Cell* 103, 399–410.
- Wang F, Dai J, Daum JR, Niedzialkowska E, Banerjee B, Stukenberg PT, Gorbisky GJ, Higgins JMG (2010). Histone H3 Thr-3 phosphorylation by Haspin positions Aurora B at centromeres in mitosis. *Science* 330, 231–235.
- Wang F, Ulyanova NP, van der Waal MS, Patnaik D, Lens SMA, Higgins JMG (2011). A positive feedback loop involving Haspin and Aurora B promotes CPC accumulation at centromeres in mitosis. *Curr Biol* 21, 1061–1069.
- Warren WD, Steffensen S, Lin E, Coelho P, Loupart M, Cobbe N, Lee JY, McKay MJ, Orr-Weaver T, Heck MM, Sunkel CE (2000). The *Drosophila* RAD21 cohesin persists at the centromere region in mitosis. *Curr Biol* 10, 1463–1466.
- Welburn JPI, Vleugel M, Liu D, Yates JR, Lampson MA, Fukagawa T, Cheeseman IM (2010). Aurora B phosphorylates spatially distinct targets to differentially regulate the kinetochore–microtubule interface. *Mol Cell* 38, 383–392.
- Wheelock MS, Wynne DJ, Tseng BS, Funabiki H (2017). Dual recognition of chromatin and microtubules by INCENP is important for mitotic progression. *J Cell Biol* 216, 925–941.
- Yamagishi Y, Yang C-H, Tanno Y, Watanabe Y (2012). MPS1/Mph1 phosphorylates the kinetochore protein KNL1/Spc7 to recruit SAC components. *Nat Cell Biol* doi:10.1038/ncb2515.
- Yamagishi Y, Honda T, Tanno Y, Watanabe Y (2010). Two histone marks establish the inner centromere and chromosome bi-orientation. *Science* 330, 239–243.
- Yue Z, Carvalho A, Xu Z, Yuan X, Cardinale S, Ribeiro S, Lai F, Ogawa H, Gudmundsdottir E, Gassmann R, et al. (2008). Deconstructing Survivin: comprehensive genetic analysis of Survivin function by conditional knockout in a vertebrate cell line. *J Cell Biol* 183, 279–296.
- Zaytsev AV, Mick JE, Maslennikov E, Nikashin B, DeLuca JG, Grishchuk EL (2015). Multisite phosphorylation of the NDC80 complex gradually tunes its microtubule-binding affinity. *Mol Biol Cell* 26, 1829–1844.
- Zuzuarregui A, Kupka T, Bhatt B, Dohnal I, Mudrak I, Friedmann C, Schüchner S, Frohner IE, Ammerer G, Ogris E (2012). M-Track: detecting short-lived protein-protein interactions in vivo. *Nat Methods* 9, 594–596.